# Computational Design of Multiple Resonance–Type BN Molecules for Inverted Singlet and Triplet Excited States

Yong-Jin Pu*[1], Danillo Valverde[2], Juan-Carlos Sancho-García*[3], Yoann Olivier*[2]

[1] RIKEN Center for Emergent Matter Science (CEMS), Wako, Saitama 351-0198, Japan. E-mail: yongjin.pu@riken.jp

[2] Laboratory for Computational Modeling of Functional Materials, Namur Institute of Structured Matter, Université de Namur, Rue de Bruxelles, 61, B-5000 Namur, Belgium.
yoann.olivier@unamur.be

[3] Department of Physical Chemistry, University of Alicante, E-03080 Alicante, Spain.
jc.sancho@ua.es

## Abstract

A computational design of linearly extended multiple resonance (MR)-type BN molecules based on DABNA-1 is proposed herein in the quest to find potential candidates that exhibit a negative singlet-triplet gap ($\Delta E_{ST}$) and a large oscillator strength. The impact of a proper account of electron correlation in the lowest singlet and triplet excited states is systematically investigated by using double-hybrid functionals within the TD-DFT framework as well as wavefunction-based methods (EOM-CCSD and SCS-CC2) since this contribution plays an essential role in driving the magnitude of the $\Delta E_{ST}$ in MR-TADF and inverted singlet-triplet gap. Our results point out to a gradual reduction of the $\Delta E_{ST}$ gap with respect to the increasing sum of the number of B and N atoms, reaching negative $\Delta E_{ST}$ values for some molecules as a function of their size. The double hybrid functionals reproduce the gap with only slight deviation compared to available experimental data for DABNA-1, ν-DABNA, and mDBCz and nicely agree with high-level quantum mechanical methods (e.g., EOM-CCSD and SCS-CC2). Larger oscillator strengths are found compared to the azaphenalene-type molecules also exhibiting the inversion of their singlet and triplet excited states. We hope this study can serve as a motivation for further design of the molecules showing negative $\Delta E_{ST}$ based on boron and nitrogen doped polyaromatic hydrocarbons.

## Introduction

An excited state control of organic molecules is important for various light-related applications such as photocatalyst, phototherapy, bioimaging, organic light-emitting diodes, organic solar cells, etc. In closed shell (standard) molecules, the ground state is a singlet ($S_0$) state and the lower-lying excited singlet state ($S_1$) is typically a bright state that decays radiatively while the lowest excited

triplet state ($T_1$) is a dark state that relaxes non-radiatively to $S_0$ at room temperature before phosphorescence takes place due to the spin selection rule. In an organic light-emitting diode (OLED), these excited states are generated upon recombination of holes and electrons injected from the electrical contacts. However, the unfavorable spin statistics leads to 25% of emissive singlet excitons and 75% of non-emissive triplet excitons, besides potentially in a low internal quantum efficiency (IQE). Thermally activated delayed fluorescence (TADF) [1] and inverted singlet-triplet gap materials (INVEST) [2] have arisen as solutions to maximize IQE by bringing in near resonance $S_1$ and $T_1$ or $T_1$ above $S_1$. Therefore, intersystem crossing (ISC) and reverse intersystem crossing (rISC) processes between $S_1$ and $T_1$ states are important to control the relative population of both $S_1$ and $T_1$ excitons, with their rate largely affected by the energy difference between $S_1$ and $T_1$, i.e., $\Delta E_{ST} = E(S_1) - E(T_1)$. In the simpler picture of two interacting electrons occupying the highest occupied molecular orbital (HOMO) and the lowest unoccupied molecular orbital (LUMO), $E(T_1)$ is lower than $E(S_1)$ by twice the exchange interaction (K) of two electrons. [3] The exchange interaction itself is by definition positive, so that it has been historically considered that $\Delta E_{ST}$ cannot be negative. However, it can be minimized by spatially separating the HOMO and LUMO orbitals to minimize orbital overlap. Such a strategy has been largely used in the TADF field.

In 1980, Leupin and Wirz reported that cyclazine, an azaphenalene molecule (molecule **1** in **Figure S1**) might show a negative $\Delta E_{ST}$ based on energy transfer experiments and the short lifetime (100 ns) recorded for $T_1$ state. [4] More recently, Domcke *et al.* performed time-resolved photoluminescence spectroscopy on a heptazine derivative (molecule **2** in **Figure S1**), a core known previously for its TADF activity which did not exhibit the usual delayed fluorescence on the µs timescale. [5-8] They also performed transient absorption and did not detect any sign of the presence of triplet state. These two sets of experiments suggested that $T_1$ would lie higher in energy with respect to $S_1$ indicating a negative $\Delta E_{ST}$ gap that was further supported by sophisticated wave function-based quantum chemical calculations. [8] Later on, researchers at RIKEN demonstrated experimentally that $HzTFEX_2$ (**Figure S1**), an heptazine derivative, exhibits a negative $\Delta E_{ST}$, and consequently a krISC rate faster than kISC rate as estimated by temperature dependent transient photoluminescence spectroscopy. [2] As the INVEST has been mostly driven by the computational chemistry community, there have been many reports on theoretical and computational design of molecules showing negative $\Delta E_{ST}$, but the molecular structures have been largely limited to the boron and/or nitrogen doped phenalene-type structures such as cyclazine and heptazine derivatives, [9-18] except a few reports of polyaromatic hydrocarbon cores (PAHs) compounds such as pentalene, COLDEM azulene-type alternant hydrocarbon molecule (compound **3** in **Figure S1**) is predicted to show a negative $\Delta E_{ST}$. [19-22]

With these precedents, it is easy to see that the expansion of the molecular design strategy (i.e., the search of new molecular cores and/or templates for further optimization with e.g. substituents) is not

only beneficial for establishing a dataset of possible candidates but is also interesting for the understanding of the underlying mechanism giving rise to a negative $\Delta E_{ST}$. Two essential ingredients are mandatory to realize negative $\Delta E_{ST}$: (i) the exchange interaction (K) should be as small as possible and (ii) electron correlation energy must stabilize $S_1$ more than $2 \cdot K$. As consequence of (ii), the $S_1$ state wavefunction should contain a larger double excitation character than the $T_1$ state wavefunction as it has been recently emphasized in the literature. [14, 18] However, so far, INVEST compounds have shown only very small oscillator strengths and thus radiative decay rates which makes them prone to non-radiative decay and potentially reduced IQE.

How can we thus design new molecules with both a negative $\Delta E_{ST}$ and a large oscillator strength? Pershin *et al.* reported that electron correlation as accounted through double excitation contribution in wavefunction-based calculations, is key to rationalize the small $\Delta E_{ST}$ of the multi-resonance TADF (MR-TADF) DABNA-1. Their $\Delta E_{ST}$ is however still positive since its HOMO and LUMO orbitals exhibit some, yet small, overlap resulting in a non-negligible exchange energy. An additional feature of MR-TADF emitters in contrast to donor-acceptor TADF emitters is their consistently large oscillator strength because of the above-mentioned non-negligible HOMO-LUMO overlap. [23] Interestingly, Pershin *et al.* also reported that $\Delta E_{ST}$ of the boron- and nitrogen-incorporated MR molecules gradually reduces as its molecular structure is linearly extended while the oscillator strength increases. [24] Inspired by these previous reports, we considered that linearly extended MR-type chemical structures will be suitable candidates, potentially exhibiting with small exchange interaction in the excited state while the inherent electron correlation effect reported for this family of compounds could help realizing negative $\Delta E_{ST}$ concomitantly with large oscillator strength which would be relevant features for real devices and/or applications.

Taken all these findings together, we here computationally designed and proposed linearly extended MR-type BN molecules inspired by the seminal work on DABNA–1, showing negative $\Delta E_{ST}$ and large oscillator strength. This finding is the main novelty of this work as it differs considerably from the previously reported azaphenalene-like and heptazine structures displaying negative $\Delta E_{ST}$ but small oscillator strength due to the high symmetry of these cores. Double hybrid time-dependent density functional theory (TD–DFT) was used in the calculations to estimate $\Delta E_{ST}$ and oscillator strength. This class of methods represents a good trade-off between accuracy and computational cost. [25-29] Wavefunction-based methods, such as the equation of motion coupled-cluster singles and doubles (EOM-CCSD) and the Spin-Component Scaling second-order approximate Coupled-Cluster (SCS-CC2), are considered for benchmarking $\Delta E_{ST}$ for smaller size systems.

## Results and Discussion

Chemical structure of the linearly extended BN ladder-type molecules is shown in **Figure 1**. The

number of B and N atoms in their molecular composition is also reported in order to facilitate the comparison of the results. $E(S_1)$ and $E(T_1)$ energies, based on vertical excitation energies (i.e., $S_0 \rightarrow S_1$ and $S_0 \rightarrow T_1$), $\Delta E_{ST}$, and oscillator strength associated with the $S_0 \rightarrow S_1$ transition of these ladder-type BN molecules are calculated with different methods and summarized in **Table 1**. The double hybrid TD-DFT with both B2PLYP and SOS-PBE-QIDH functionals give an expected smaller $\Delta E_{ST}$ than TD-DFT with B3LYP in all molecules, as a result from the inclusion of the double excitation contribution in double-hybrid functionals. $\Delta E_{ST}$ with any of the employed functionals gradually decreases upon increasing the molecular size to the point of becoming negative in the case of the double hybrid functionals. The most negative $\Delta E_{ST}$ value is estimated to be –0.086 eV for B9N9 system using SOS-PBE-QIDH functional. Basis set effects going from the cost-effective cc-pVDZ to cc-pVTZ were also evaluated using SOS-PBE-QIDH functional as the reference, resulting in negligible changes (e.g., differences for $\Delta E_{ST}$ less than 0.01 eV for B1N2, B2N1, B2N2, B2N3, and B3N2 taken as benchmark set) (**Table S1**). Based on these findings, the cc-pVDZ basis set is kept for the remaining calculations presented here, allowing the study of considerably large molecules.

As shown in **Figure S2a**, when $\Delta E_{ST}$ is plotted vs the number of π-electrons in the molecule, a clear decreasing trends appear, but some small opposite-trends also emerges periodically between the two molecules of which the sum of the number of B and N atoms are the same, for example, B1N2 and B2N1, B2N3 and B3N2, etc. This is rationalized because the contribution of N to the extension of π-conjugation is larger than the contribution of B due to the lone pair electrons in N. Therefore, the plot of $\Delta E_{ST}$ vs the sum of the number of B and N would not remove the small opposite-trends appearing in the plot (see **Figure S2b**); however, when $\Delta E_{ST}$ is plotted vs the sum of the number of B and half of the number of N (see **Figure 2**), the small periodical opposite-trends disappeared and the decreasing trend of $\Delta E_{ST}$ becoming much smoother. The curve fitting of $\Delta E_{ST}$ to the number of [B + N/2] using the inversely proportional formula $y = a/x + b$ showed a high correlation with the R-squared ($R^2$) values above 97% (**Table 2**). Extrapolated $\Delta E_{ST}$ values by the fitting are 0.091 eV from B3LYP, –0.113 eV from B2PLYP, and –0.138 eV from SOS-PBE-QIDH.

The experimental $\Delta E_{ST}$ value of B1N2 (DABNA-1) is reported to be 0.15 eV[30] and plotted as a black circle in **Figure 2**. The double-hybrid TD-DFT calculations showed much smaller error (small overestimation by 0.05–0.07 eV) for B1N2 to the experimental value than B3LYP does because of the poor account of electron correlation and are in line with the SCS-CC2 results which we demonstrated as method of choice for predicting $\Delta E_{ST}$ of MR-TADF materials with deviation in $\Delta E_{ST}$ of 0.03 and 0.06 eV for B2PLYP and SOS-PBE-QIDH, respectively. Among double-hybrid functionals tested on azaphenalene molecules,[27-29] SOS-PBE-QIDH has been reported as one of the most reliable functionals when predicting a negative $\Delta E_{ST}$ in this family of compounds. We also calculated two azaphenalene molecules synthesized by the RIKEN researchers reported to have

experimental $\Delta E_{ST}$ that amounts to –0.011 eV for $HzTFEX_2$ and 0.052 eV for $HzPipX_2$ (**Table S2**).[2] However, both double hybrid functionals, B2PLYP and SOS-PBE-QIDH, give overestimated negative $\Delta E_{ST}$ with errors with respect to the experiments ranging from –0.170 eV to –0.277 eV. Interestingly, neither EOM-CCSD nor SCS-CC2 methods are also able to predict a positive $\Delta E_{ST}$ for $HzPipX_2$ (**Table S2**). On the other hand, for comparison, we investigated the relatively large and actually synthesized BN-type molecule, ν-DABNA and mDBCz, whose experimental $\Delta E_{ST}$ was reported to be as small as 0.017 eV[31] and 0.040 eV[32], respectively (**Table S2**). We obtained $\Delta E_{ST}$ of 0.057 eV from B2PLYP and 0.028 eV from SOS-PBE-QIDH for ν-DABNA and $\Delta E_{ST}$ of 0.029 eV from B2PLYP and –0.118 eV from SOS-PBE-QIDH for mDBCz. Overall, we observed that B2PLYP leads to a good agreement with the experiments and SCS-CC2 calculations. We should remark that molecules larger than B1N2, among the calculated molecules in this study, remain predictions since they have not been synthesized so far. Interestingly, the longer BN ladder-type molecules follow the obtained decreasing trend toward negative $\Delta E_{ST}$ values as predicted by the double hybrid TD-DFT methods, mainly resulting from a decrease in the exchange energy. A proper account of correlation effect remains quite tricky so that the prediction of negative $\Delta E_{ST}$ should be cross-compared between different computational methods. However as mentioned above, wavefunction-based methods are not accessible for the full range of systems, therefore we must also consider the possibility that the computationally predicted negative $\Delta E_{ST}$ of the BN ladder-type molecules would lie within the error bar of the methods possibly resulting in an actual slightly positive $\Delta E_{ST}$. Likely, we expect that the magnitude of the error would not be systematic and would depend on the systems size. Still, if we consider the error obtained for the $\Delta E_{ST}$ of DABNA-1 with the B2PLYP and SOS-PBE-QIDH double-hybrid functionals, B9N9 would thus result in a positive $\Delta E_{ST}$.

To summarize briefly, the double hybrid TD-DFT calculations lead to the following results: 1) $\Delta E_{ST}$ was underestimated for the azaphenalene molecules, $HzTFEX_2$ and $HzPipX_2$, by an error from –0.170 eV to –0.277 eV; 2) $\Delta E_{ST}$ was overestimated for the BN molecules, DABNA-1 and ν-DABNA, by the error from 0.011 eV to 0.072 eV, and underestimated for mDBCz by the error from –0.011 eV to –0.158 eV. We still cannot rule out the possibility that the quality of the double-hybrid functional largely depends on the type and/or size of molecules due to the lack of experimental data on related molecules. Additionally, we can neither rule out the influence of dynamic and/or polarization effects[33] on the experimental values, which could further influence the comparison between theoretical and experimental results.

Perusing into the results obtained by double-hybrid functionals, the perturbative correction (D) of the $S_1$ state is as expected larger than that of $T_1$ state, or in other words, the double excitations contribution is more pronounced in the $S_1$ than in the $T_1$ state (**Figure 3**). The (D) values for the $S_1$ state obtained with B2PLYP and SOS-PBE-QIDH are very similar, but for the $T_1$ state, SOS-PBE-

QIDH showed smaller (D) values than B2PLYP. The (D) correction in the $S_1$ state, is less dependent on the extension of π-conjugation than for the $T_1$ state. Furthermore, the (D) correction in the $S_1$ state is minimized for B3N3 and slightly increases for longer compounds. A potential explanation could be that the $S_1$ electronic density is so spread upon the extension of π-conjugation that the correlation effects are slightly weaker. Besides, the (D) value of the $T_1$ state gradually becomes more negative with the extension of π-conjugation, and approaches a constant value, indicating that even $T_1$ can have a certain double excitation character with increasing the π-conjugation. The constant value of the $T_1$ (D) value might arise from the stronger localization of the triplet state in comparison to $S_1$.

Oscillator strengths (*f*) increase with the extension of π-conjugation, and the sum of the number of B and half of the number of N also shows a better correlation than the number of π-electrons (**Figure S3**). The increase of oscillator strength with the extension of π-conjugation can be attributed to increase of polarizability in the extended systems. This is very much in line with the work of Vezie et al. that reported that the oscillator strength of several π-conjugated oligomers normalized by the number of π-electrons in the system increases due to the superlinear increase of the polarizability with the increase of the number of π-electrons. [34] The BN molecules in this study also exhibit a same trend (**Figure 4**), since the transition dipole moment of the $S_1$ state is aligned with the long axis of the molecules. Consequently, relative large oscillator strength values can be achieved concomitantly with negative $\Delta E_{ST}$. This is a finding totally different from the previously reported negative $\Delta E_{ST}$ compounds, such as azaphenalene and fused alternant hydrocarbons[8, 9, 17], and could pave the way towards reliable devices and/or further applications.

In addition to the linearly extended BN molecules, the $\Delta E_{ST}$ and the oscillator strengths of a set of topologically different (zigzag-, circulene-, and graphene-type) BN molecules were also calculated with double-hybrid TD-DFT methods (**Figure 5** and **Table 3**). The zigzag-type BN molecules also showed negative $\Delta E_{ST}$ and large oscillator strength. In addition, we predicted largely negative $\Delta E_{ST}$ for circulene- and graphene-type molecules that amounts to –0.153 eV for B9N9_C and –0.269 eV for B12N12_G with the SOS-PBE-QIDH functional, but their oscillation strength is zero likely originating from the high symmetry point group of these compounds.

## Conclusions

We designed a large set of linearly extended MR-type BN molecules inspired by the DABNA–1 MR-TADF emitter, which computationally showed negative $\Delta E_{ST}$ and large oscillator strength, based on B2PLYP and SOS-PBE-QIDH double-hybrid functionals calculations that are able to introduce electron correlation effect into excited-states of any multiplicity through a second-order perturbative correction. The gradual decrease of $\Delta E_{ST}$ to achieve a negative $\Delta E_{ST}$ value displayed a high correlation with the increasing sum of the number of B and half N atoms in the molecular structure,

which is a key result for the molecular design strategy. The double-hybrid functionals selected reproduced the experimental $\Delta E_{ST}$ of DABNA-1, ν-DABNA, and mDBCz with only slight deviations and provide a good agreement with more robust wavefunction-based approaches (EOM-CCSD and SCS-CC2). Nonetheless, we still cannot deny the possibility that these methods overestimated $\Delta E_{ST}$ (i.e., predicted to be too negative) of the most extended BN molecules. It is extremely hard to actually synthesize the extended BN molecules, so that the verification of the negative $\Delta E_{ST}$ is now pending. Another key result is that these extended BN molecules, while showing negative $\Delta E_{ST}$ values, display relatively large oscillator strengths in contrast to the azaphenalene molecules that were identified as INVEST materials. Finally, the molecular design followed in this study will help to widen the set of molecules for which a negative $\Delta E_{ST}$ is predicted, and to consequently develop INVEST emitter with a high radiative decay rate molecules efficient triplet-harvesting abilities for OLED applications.

**Acknowledgments**

J.C.S.G. acknowledges financial support from the "Ministerio de Ciencia e Innovación" of Spain (project PID2019-106114GB-I00). D.V and Y.O. acknowledges funding by the "Fonds de la Recherche Scientifique-FNRS" under Grant no. F.4534.21 (MIS-IMAGINE). The work in Namur has been funded by the Belgian National Fund for Scientific Research (F.R.S.-FNRS) within the Consortium des Équipements de Calcul Intensif (CÉCI), under Grant No. 2.5020.11. The present research benefited from computational resources made available on the HOKUSAI Big Waterfall system at RIKEN and Lucia, the Tier-1 supercomputer of the Walloon Region, infrastructure funded by the Walloon Region under the grant agreement n°1910247.

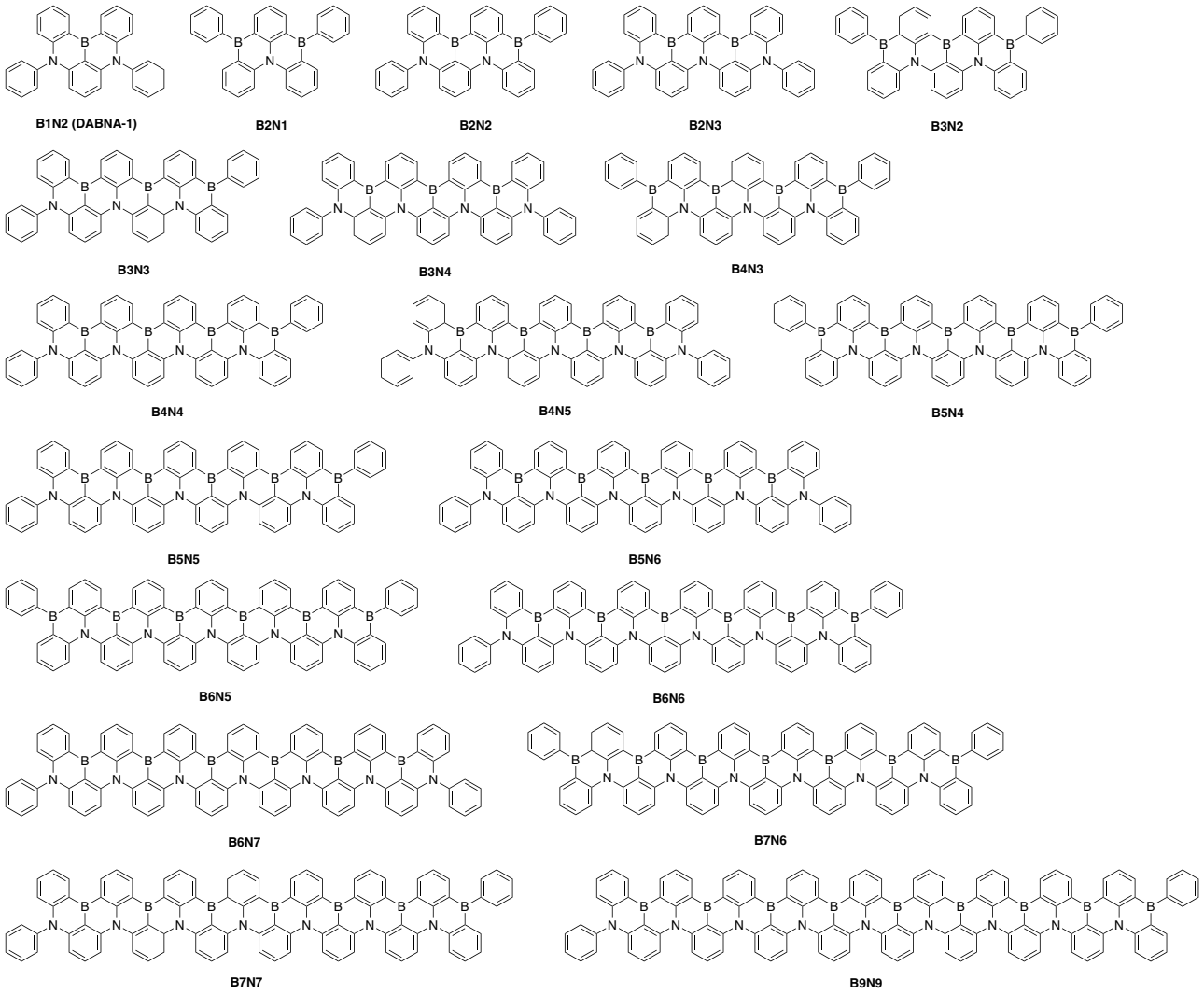


**Figure 1**. Chemical structures of the ladder-type BN molecules.

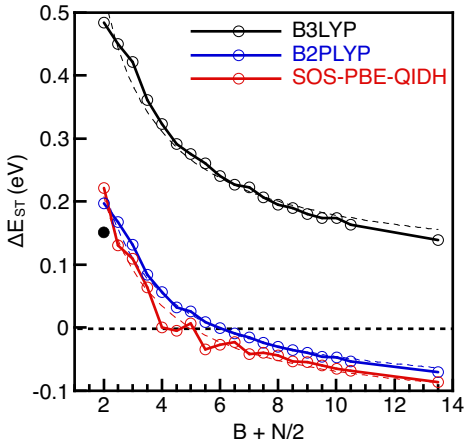


**Figure 2**. $\Delta E_{ST}$ plotted vs sum of the number of B and half N. The black circle represents the experimental $\Delta E_{ST}$ of B1N2 (DABNA-1) as 0.15 eV. The dotted lines are a curve fitting line.

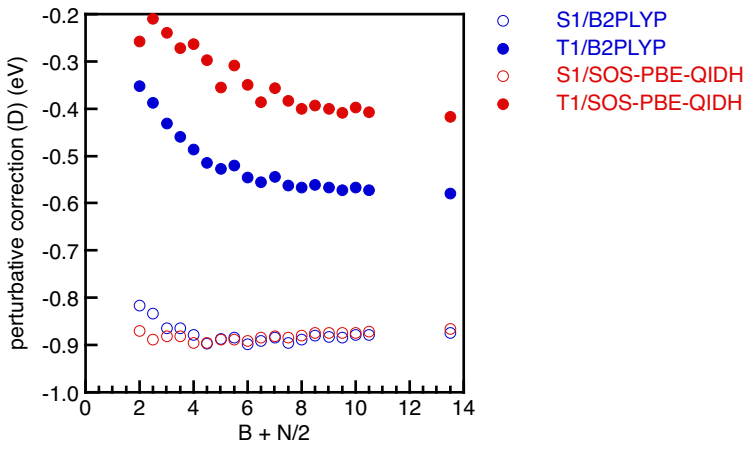


**Figure 3**. Double-hybrid functional perturbative correction (D) as a function of the sum of the number of B and half of N.

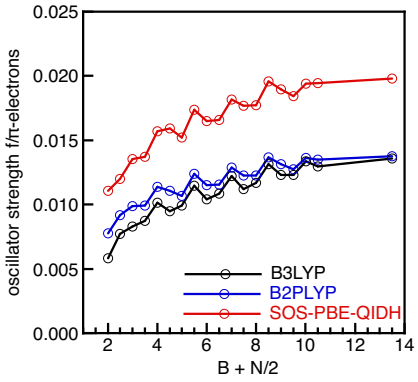


**Figure 4**. Oscillator strength computed at the TD-DFT level normalized by the number of π-electrons as a function of the sum of the number of B and half of N.

**Table 1**. Vertical excitation energies (eV), oscillator strength (f) , and $\Delta E_{ST}$ of the ladder-type BN molecules, as calculated with different methods.

| | N(e)[b] | B+N[c] | B+N/2[d] | B3LYP[a] | | | | B2PLYP[a] | | | | SOS-PBE-QIDH[a] | | | |
|---|---|---|---|---|---|---|---|---|---|---|---|---|---|---|---|
| | | | | $E(S_1)$[e] | f/N[f] | $E(T_1)$[e] | $\Delta E_{ST}$ | $E(S_1)$[e] | f/N[f] | $E(T_1)$[e] | $\Delta E_{ST}$ | $E(S_1)$[e] | f/N[f] | $E(T_1)$[e] | $\Delta E_{ST}$ |
| B1N2 | 34 | 3 | 2.0 | 3.083 | 0.0058 | 2.598 | 0.484 | 2.753 | 0.0078 | 2.556 | 0.197 | 3.245 | 0.0111 | 3.023 | 0.222 |
| B2N1 | 32 | 3 | 2.5 | 2.955 | 0.0077 | 2.504 | 0.450 | 2.601 | 0.0091 | 2.433 | 0.168 | 3.111 | 0.0120 | 2.980 | 0.131 |
| B2N2 | 40 | 4 | 3.0 | 2.729 | 0.0083 | 2.308 | 0.421 | 2.361 | 0.0099 | 2.229 | 0.132 | 2.925 | 0.0135 | 2.816 | 0.109 |
| B2N3 | 48 | 5 | 3.6 | 2.610 | 0.0087 | 2.249 | 0.361 | 2.233 | 0.0099 | 2.149 | 0.084 | 2.811 | 0.0137 | 2.747 | 0.064 |
| B3N2 | 46 | 5 | 4.0 | 2.599 | 0.0101 | 2.276 | 0.323 | 2.215 | 0.0114 | 2.159 | 0.056 | 2.810 | 0.0157 | 2.810 | 0.000 |
| B3N3 | 54 | 6 | 4.5 | 2.494 | 0.0095 | 2.203 | 0.292 | 2.110 | 0.0111 | 2.078 | 0.032 | 2.736 | 0.0159 | 2.741 | –0.005 |
| B3N4 | 62 | 7 | 5.0 | 2.375 | 0.0099 | 2.100 | 0.276 | 1.982 | 0.0107 | 1.956 | 0.026 | 2.598 | 0.0152 | 2.591 | 0.007 |
| B4N3 | 60 | 7 | 5.5 | 2.405 | 0.0115 | 2.145 | 0.261 | 2.018 | 0.0124 | 2.009 | 0.009 | 2.636 | 0.0174 | 2.670 | –0.034 |
| B4N4 | 68 | 8 | 6.0 | 2.321 | 0.0104 | 2.080 | 0.241 | 1.932 | 0.0115 | 1.933 | –0.001 | 2.569 | 0.0165 | 2.596 | –0.027 |
| B4N5 | 76 | 9 | 6.5 | 2.274 | 0.0109 | 2.047 | 0.227 | 1.882 | 0.0115 | 1.891 | –0.009 | 2.515 | 0.0166 | 2.538 | –0.023 |
| B5N4 | 74 | 9 | 7.0 | 2.300 | 0.0122 | 2.077 | 0.223 | 1.912 | 0.0129 | 1.927 | –0.015 | 2.541 | 0.0182 | 2.583 | –0.042 |
| B5N5 | 81 | 10 | 7.5 | 2.245 | 0.0112 | 2.039 | 0.206 | 1.859 | 0.0122 | 1.883 | –0.024 | 2.504 | 0.0177 | 2.544 | –0.040 |
| B5N6 | 90 | 11 | 8.0 | 2.217 | 0.0117 | 2.021 | 0.195 | 1.830 | 0.0122 | 1.860 | –0.030 | 2.470 | 0.0177 | 2.514 | –0.044 |
| B6N5 | 88 | 11 | 8.5 | 2.220 | 0.0131 | 2.031 | 0.190 | 1.836 | 0.0137 | 1.872 | –0.036 | 2.471 | 0.0196 | 2.524 | –0.053 |
| B6N6 | 96 | 12 | 9.0 | 2.197 | 0.0123 | 2.017 | 0.181 | 1.817 | 0.0131 | 1.857 | –0.040 | 2.457 | 0.0190 | 2.512 | –0.055 |
| B6N7 | 104 | 13 | 9.5 | 2.182 | 0.0123 | 2.008 | 0.174 | 1.799 | 0.0128 | 1.845 | –0.046 | 2.441 | 0.0184 | 2.501 | –0.060 |
| B7N6 | 102 | 13 | 10.0 | 2.198 | 0.0133 | 2.024 | 0.174 | 1.815 | 0.0136 | 1.862 | –0.047 | 2.454 | 0.0194 | 2.519 | –0.065 |
| B7N7 | 110 | 14 | 10.5 | 2.172 | 0.0130 | 2.008 | 0.164 | 1.793 | 0.0135 | 1.846 | –0.053 | 2.434 | 0.0194 | 2.502 | –0.068 |
| B9N9 | 138 | 18 | 13.5 | 2.134 | 0.0136 | 1.995 | 0.139 | 1.759 | 0.0138 | 1.829 | –0.070 | 2.402 | 0.0198 | 2.488 | –0.086 |

a) With the cc-pVDZ basis set. b) The number of π-electrons. c) Sum of the number of B atoms and the number of N atoms. d) Sum of the number of B atoms and half the number of N atoms. e) Vertical excitation energy at $S_0 \rightarrow S_1$ and $S_0 \rightarrow T_1$. f) Oscillator strength normalized by the number of π-electrons associated with the $S_0 \rightarrow S_1$ transition.

**Table 2**. $\Delta E_{ST}$ (eV) value obtained by extrapolation of the fitting curve and coefficient of determination.

| | π-electrons | | B + N | | B + N/2 | |
|---|---|---|---|---|---|---|
| | $\Delta E_{ST}$ | $R^2$ | $\Delta E_{ST}$ | $R^2$ | $\Delta E_{ST}$ | $R^2$ |
| B3LYP | 0.031 | 0.9767 | 0.087 | 0.9760 | 0.091 | 0.9734 |
| B2PLYP | –0.157 | 0.9712 | –0.116 | 0.9857 | –0.113 | 0.9868 |
| SOS-PBE-QIDH | –0.175 | 0.8735 | –0.138 | 0.9238 | –0.138 | 0.9739 |

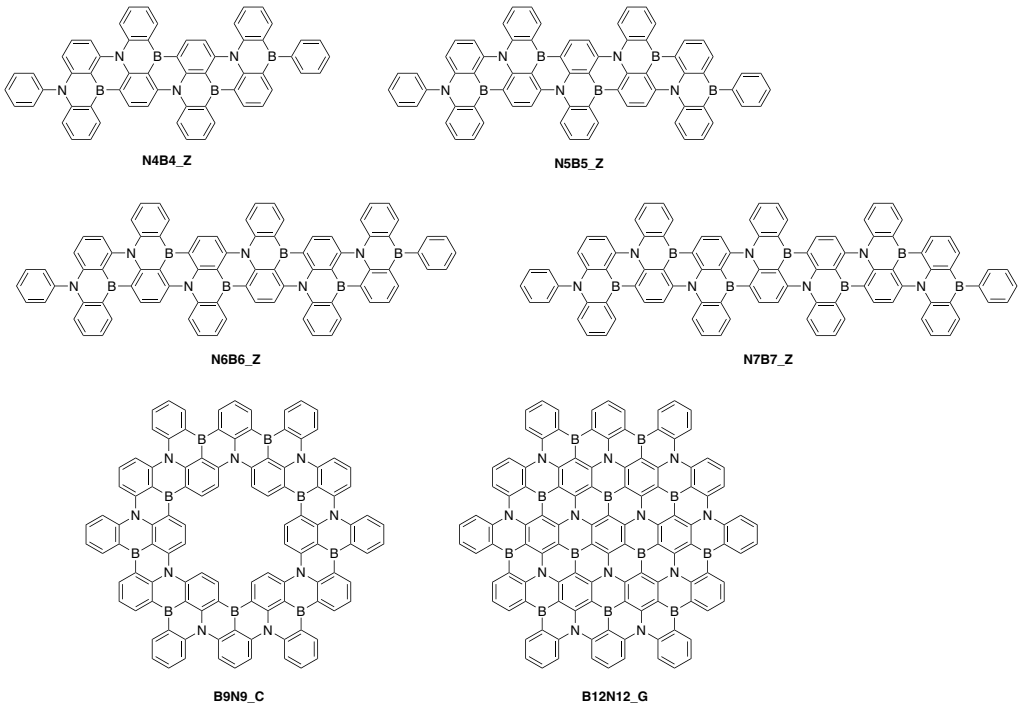


**Figure 5**. Chemical structure of the zigzag-, circulene-, and graphene-type BN molecules.

**Table 3**. Vertical excitation energies (eV), oscillator strength, and $\Delta E_{ST}$ values of the zigzag- and circulene-type BN molecules, as calculated with different methods.

| | N(e)[b] | B+N[c] | B+N/2[d] | B3LYP[a] | | | | B2PLYP[a] | | | | SOS-PBE-QIDH[a] | | | |
|---|---|---|---|---|---|---|---|---|---|---|---|---|---|---|---|
| | | | | $S_1 \leftarrow S_0$[e] | f/N[f] | $T_1 \leftarrow S_0$[e] | $\Delta E_{ST}$ | $S_1 \leftarrow S_0$[e] | f/N[f] | $T_1 \leftarrow S_0$[e] | $\Delta E_{ST}$ | $S_1 \leftarrow S_0$[e] | f/N[f] | $T_1 \leftarrow S_0$[e] | $\Delta E_{ST}$ |
| B4N4_Z | 68 | 8 | 6 | 2.327 | 0.0073 | 2.103 | 0.224 | 1.970 | 0.0106 | 1.995 | –0.025 | 2.650 | 0.0166 | 2.674 | –0.024 |
| B5N5_Z | 82 | 10 | 7.5 | 2.269 | 0.0073 | 2.089 | 0.180 | 1.931 | 0.0120 | 1.984 | –0.053 | 2.623 | 0.0188 | 2.678 | –0.055 |
| B6N6_Z | 96 | 12 | 9 | 2.238 | 0.0071 | 2.085 | 0.154 | 1.918 | 0.0131 | 1.982 | –0.064 | 2.603 | 0.0201 | 2.676 | –0.073 |
| B7N7_Z | 110 | 14 | 10.5 | 2.225 | 0.0068 | 2.087 | 0.138 | 1.915 | 0.0137 | 1.984 | –0.069 | 2.590 | 0.0204 | 2.676 | –0.086 |
| B3N3_C | 48 | 6 | 4.5 | 2.975 | 0.0000 | 2.643 | 0.331 | 2.611 | 0.0000 | 2.706 | –0.095 | 3.139 | 0.0000 | 3.248 | –0.109 |
| B9N9_C | 126 | 18 | 13.5 | 2.054 | 0.0000 | 1.946 | 0.108 | 1.705 | 0.0000 | 1.819 | –0.114 | 2.331 | 0.0000 | 2.484 | –0.153 |
| B12N12_G | 138 | 24 | 18 | 2.411 | 0.0000 | 2.264 | 0.146 | 1.993 | 0.0000 | 2.150 | –0.157 | 2.715 | 0.0000 | 2.984 | –0.269 |

a) With the cc-pVDZ basis set. b) The number of π-electrons. c) Sum of the number of B atoms and the number of N atoms. d) Sum of the number of B atoms and half the number of N atoms. e) Vertical excitation energy at $S_0 \rightarrow S_1$ and $S_0 \rightarrow T_1$. f) Oscillator strength normalized by the number of π-electrons associated with the $S_0 \rightarrow S_1$ transition.

## References


1. H. Uoyama, K. Goushi, K. Shizu, H. Nomura and C. Adachi, *Nature*, 2012, **492**, 234.
2. N. Aizawa, Y.-J. Pu, Y. Harabuchi, A. Nihonyanagi, R. Ibuka, H. Inuzuka, B. Dhara, Y. Koyama, K. Nakayama, S. Maeda, F. Araoka and D. Miyajima, *Nature*, 2022, **609**, 502.
3. A. D. Becke, *J. Chem. Phys.*, 2018, **148**, 44112.
4. W. Leupin and J. Wirz, *J. Am. Chem. Soc.*, 1980, **102**, 6068.
5. J. Li, T. Nakagawa, J. MacDonald, Q. S. Zhang, H. Nomura, H. Miyazaki and C. Adachi, *Adv. Mater.*, 2013, **25**, 3319.
6. J. Li, Q. S. Zhang, H. Nomura, H. Miyazaki and C. Adachi, *Appl. Phys. Lett.*, 2014, **105**, 13301.
7. J. Li, H. Nomura, H. Miyazaki and C. Adachi, *Chem. Commun.*, 2014, **50**, 6174.
8. J. Ehrmaier, E. J. Rabe, S. R. Pristash, K. L. Corp, C. W. Schlenker, A. L. Sobolewski and W. Domcke, *J. Phys. Chem. A*, 2019, **123**, 8099.
9. P. de Silva, *J. Phys. Chem. Lett.*, 2019, **10**, 5674.
10. G. Ricci, E. San-Fabian, Y. Olivier and J. C. Sancho-Garcia, *ChemPhysChem*, 2021, **22**, 553.
11. K. Bhattacharyya, *Chem. Phys. Lett.*, 2021, **779**, 5.
12. S. Pios, X. Huang, A. L. Sobolewski and W. Domcke, *Phys. Chem. Chem. Phys.*, 2021, **23**, 12968.
13. R. Pollice, P. Friederich, C. Lavigne, G. D. Gomes and A. Aspuru-Guzik, *Matter*, 2021, **4**, 1654.
14. J. Sanz-Rodrigo, G. Ricci, Y. Olivier and J. C. Sancho-Garcia, *J. Phys. Chem. A*, 2021, **125**, 513.
15. F. Dinkelbach, M. Bracker, M. Kleinschmidt and C. M. Marian, *J. Phys. Chem. A*, 2021, **125**, 10044.
16. A. L. Sobolewski and W. Domcke, *J. Phys. Chem. Lett.*, 2021, **12**, 6852.
17. G. Ricci, J. C. Sancho-Garcia and Y. Olivier, *J. Mater. Chem. C*, 2022, **10**, 12680.
18. L. Tuckova, M. Straka, R. R. Valiev and D. Sundholm, *Phys. Chem. Chem. Phys.*, 2022, **24**, 18713.
19. S. Koseki, T. Nakajima and A. Toyota, *Can. J. Chem.*, 1985, **63**, 1572.
20. A. Toyota and T. Nakajima, *J. Chem. Soc. Perkin Trans. 2*, 1986, 1731.
21. A. Toyota, *Theor. Chim. Acta*, 1988, **74**, 209.
22. J. T. Blaskovits, M. H. Garner and C. Corminboeuf, *Angew. Chem. Int. Ed.*, 2023, **62**, e202218156.
23. D. Hall, J. C. Sancho-Garcia, A. Pershin, G. Ricci, D. Beljonne, E. Zysman-Colman and Y. Olivier, *J. Chem. Theory Comput.*, 2022, **18**, 4903.
24. A. Pershin, D. Hall, V. Lemaur, J. C. Sancho-Garcia, L. Muccioli, E. Zysman-Colman, D. Beljonne and Y. Olivier, *Nat. Commun.*, 2019, **10**, 597.
25. S. Grimme, *J. Chem. Phys.*, 2006, **124**, 34108.
26. S. Grimme and F. Neese, *J. Chem. Phys.*, 2007, **127**, 154116.
27. J. C. Sancho-Garcia, E. Bremond, G. Ricci, A. J. Perez-Jimenez, Y. Olivier and C. Adamo, *J. Chem. Phys.*, 2022, **156**, 34105.
28. M. Kondo, *Chem. Phys. Lett.*, 2022, **804**, 139895.
29. M. Alipour and T. Izadkhast, *J. Chem. Phys.*, 2022, **156**, 64302.
30. T. Hatakeyama, K. Shiren, K. Nakajima, S. Nomura, S. Nakatsuka, K. Kinoshita, J. P. Ni, Y. Ono and T. Ikuta, *Adv. Mater.*, 2016, **28**, 2777.
31. Y. Kondo, K. Yoshiura, S. Kitera, H. Nishi, S. Oda, H. Gotoh, Y. Sasada, M. Yanai and T. Hatakeyama, *Nat. Photon.*, 2019, **13**, 678.
32. X. L. Cai, Y. X. Pu, C. L. Li, Z. H. Wang and Y. Wang, *Angew. Chem. Int. Ed.*, 2023, **62**, e202304104.
33. Y. Olivier, B. Yurash, L. Muccioli, G. D'Avino, O. Mikhnenko, J. C. Sancho-Garcia, C. Adachi, T. Q. Nguyen and D. Beljonne, *Phy. Rev. Mater.*, 2017, **1**, 75602.
34. M. S. Vezie, S. Few, I. Meager, G. Pieridou, B. Dorling, R. S. Ashraf, A. R. Goni, H. Bronstein,

I. McCulloch, S. C. Hayes, M. Campoy-Quiles and J. Nelson, *Nat. Mater.*, 2016, **15**, 746.

# Supporting Information

## Methodology

All ground-state molecular structures were optimized at the B3LYP/cc-pVDZ level and showed positive frequencies. First estimate of the excitation energies at the same level was performed with employing Time-Dependent Density-Functional Theory (TD-DFT). TD-DFT with the B2PLYP[1, 2] and SOS-PBE-QIDH[3] double hybrid functionals was also employed since it considers electron correlation and double excitation effects in its implementation. These expressions incorporate the electron correlation effect by adding a second-order Møller–Plesset perturbation theory (MP2) contribution to Hartree-Fock (HF) exchange and standard generalized gradient approximations (GGAs) for exchange and for correlation, as for the B2PLYP case.

$$E_{XC}^{B2PLYP} = c_x E_X^{HF} + (1 - c_x)E_X^{B88\ GGA} + (1 - c_c)E_C^{LYP\ GGA} + c_c E_C^{MP2} \quad (1)$$

$\Delta E_{ST}$ can be then estimated by computing the corresponding vertical excitation energies that can be formally written as the sum of the conventional TD-DFT and configuration interaction singles with perturbative doubles (CIS(D)) corrections, with the latter term responsible for taking into account the electron correlation effect, corresponding to the ground state MP2 correction.

$$\Delta E^{B2PLYP}(c_x, c_c) = \Delta E^{TD\text{-}DFT}(c_x, c_c) + c_c \Delta E^{CIS(D)} \quad (2)$$

Originally, weights of 0.53 and 0.27 have been used for $c_x$ and $c_c$, respectively, for the B2PLYP functional. Recently, Kondo reported that 0.40 for $c_x$ gave a closer $\Delta E_{ST}$ for DABNA-1 to its experimental value, while $c_c$ remained at its original value of 0.27.[4] In this study, the set ($c_x$, $c_c$) = (0.40, 0.27) was used for B2PLYP functional to allow comparison with previously reported results in literature for DABNA-1.

SOS-PBE-QIDH is a spin-opposite-scaled (SOS) version of the quadratic integrand double-hybrid (QIDH) functional that also incorporates as ingredients HF and PBE exchange, as well as MP2 and PBE correlation, using the following expression:

$$E_{XC}^{PBE\text{-}QIDH} = [(\lambda + 2)/3]E_X^{HF} + [(1 - \lambda)/3]E_X^{PBE\ GGA} + (2/3)E_C^{PBE\ GGA} + (1/3)E_C^{MP2} \quad (3)$$

with $\lambda = 3^{2/3} - 2$.[5]

In the vertical excitation energies calculation, $E_C^{CIS(D)}$ is separated into direct and indirect terms as follows:

$$E^{CIS(D)} = \langle \Phi_{CIS} | \hat{V} | \hat{U}_2 \Phi_0 \rangle + \langle \Phi_{CIS} | \hat{V} | \hat{T}_2 \hat{U}_1 \Phi_0 \rangle \quad (4)$$

where $\hat{U}_2$ and $\hat{U}_1$ are the operators generating the doubly and singly excited wave functions from the HF determinant ($\Phi_0$), respectively. $\hat{T}_2$ is the operator generating the double excitation of two inactive electrons, $\hat{V}$ is a perturbation potential, and $\Phi_{CIS}$ is the CIS wave function. The electron pair contributions in the excitation can be divided into opposite-spin (OS) and same-spin (SS) contributions to be weighed differently. The two terms in equation (4) are broken down into opposite- and same-spin components.

$$E^{CIS(D)} = \langle \Phi_{CIS} | \hat{V} | (C_U^{OS} \hat{U}_2 + C_U^{SS} \hat{U}_2) \Phi_0 \rangle + \langle \Phi_{CIS} | \hat{V} | (C_T^{OS} \hat{T}_2 + C_T^{SS} \hat{T}_2) \hat{U}_1 \Phi_0 \rangle \quad (5)$$

where $C_U^{OS}$ and $C_U^{SS}$ are, respectively, the opposite- and same-spin scale parameters for the direct term, and $C_T^{OS}$ and $C_T^{SS}$ are, respectively, the related parameters for the indirect term. By setting the same-spin scale parameters to zero, i.e., $C_U^{SS} = 0$ and $C_T^{SS} = 0$, one recovers the original SOS-CIS(D) method.

$$E^{SOS\text{–}CIS(D)} = \langle \Phi_{CIS} | \hat{V} | C_U^{OS} \hat{U}_2 \Phi_0 \rangle + \langle \Phi_{CIS} | \hat{V} | C_T^{OS} \hat{T}_2 \hat{U}_1 \Phi_0 \rangle \quad (6)$$

However, for the SOS-PBE-QIDH case, $C_T^{OS} = 0.5470$ and $C_U^{OS} = 0.5730$ are obtained by fitting to excited-state datasets and will be thus used also here.

As reference and sanity check, equation-of-motion coupled-cluster singles and doubles (EOM-CCSD) and second-order approximate coupled cluster singles and doubles with the spin-component scaled correction (SCS-CC2) approaches were also employed for some of the smallest systems. EOM-CCSD calculations were done with Q-Chem 5.3.0, [6] while SCS-CC2 calculations were performed with TURBOMOLE 7.5. [7] Double hybrid TD-DFT calculations with B2PLYP and SOS-PBE-QIDH were performed with ORCA 5.0.3. [8] TD-DFT calculation with B3LYP was performed with Gaussian 16 RevC.01. All these calculations were carried out using the double-zeta dunning basis set (cc-pVDZ). [9]

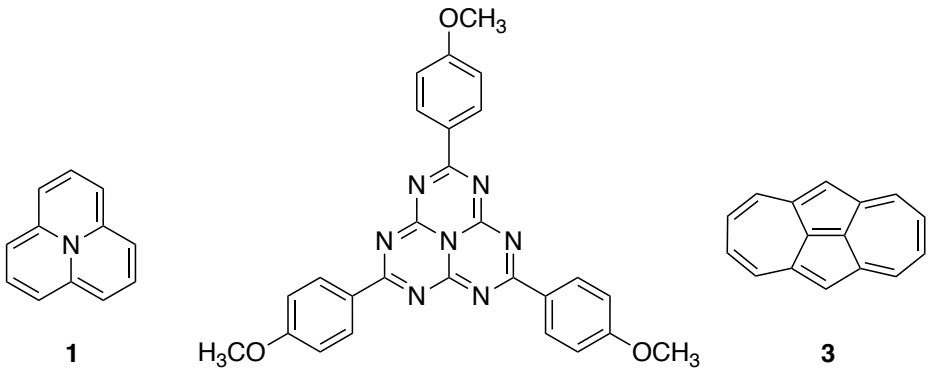

**1** **2** **3**

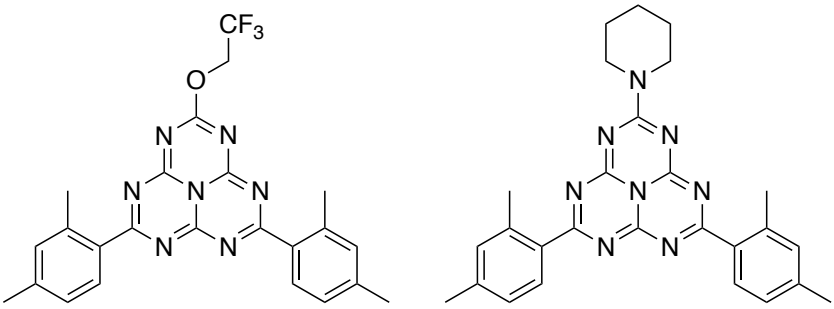

**HzTFEX$_2$** **HzPipX$_2$**

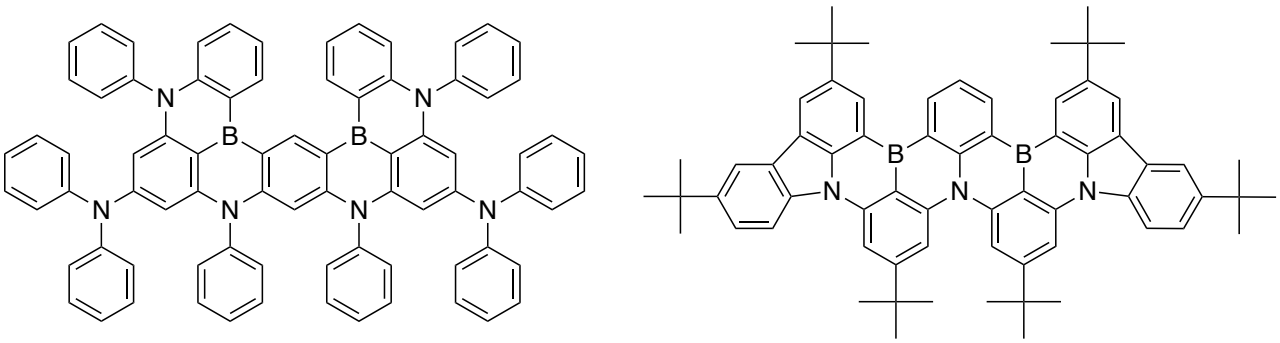

**v-DABNA** **mDBCz**

**Figure S1**. Chemical structures of the previously reported compounds.

**Table S1**. Vertical excitation energies (eV) and $\Delta E_{ST}$ of B1N2, B2N1, B2N2, B2N3, B3N2 with the cc-pVTZ basis set

| | SOS-PBE-QIDH | | |
|---|---|---|---|
| | $E(S_1)^{a)}$ | $E(T_1)^{a)}$ | $\Delta E_{ST}$ |
| B1N2 | 3.196 | 2.983 | 0.213 |
| B2N1 | 3.078 | 2.947 | 0.131 |
| B2N2 | 2.891 | 2.785 | 0.106 |
| B2N3 | 2.774 | 2.713 | 0.061 |
| B3N2 | 2.780 | 2.773 | 0.007 |

a) Vertical excitation energy at $S_0 \rightarrow S_1$ and $S_0 \rightarrow T_1$.

**Table S2**. Vertical excitation energies (eV), oscillator strength (f), and $\Delta E_{ST}$ of smaller size molecules at the EOM-CCSD and SCS-CC2 levels of theory.

| | exp | EOM-CCSD[a)] | | | | SCS-CC2[a)] | | | | B2PLYP | | | | SOS-PBE-QIDH | | | |
|---|---|---|---|---|---|---|---|---|---|---|---|---|---|---|---|---|---|
| | $\Delta E_{ST}$ | $E(S_1)^{b)}$ | $f^{c)}$ | $E(T_1)^{b)}$ | $\Delta E_{ST}$ | $E(S_1)^{b)}$ | $f^{c)}$ | $E(T_1)^{b)}$ | $\Delta E_{ST}$ | $E(S_1)^{b)}$ | $f^{c)}$ | $E(T_1)^{b)}$ | $\Delta E_{ST}$ | $E(S_1)^{b)}$ | $f^{c)}$ | $E(T_1)^{b)}$ | $\Delta E_{ST}$ |
| $HzTFEX_2$ | –0.011 | 3.136 | 0.021 | 3.252 | -0.116 | 3.039 | 0.024 | 3.382 | -0.285 | 2.579 | 0.028 | 2.855 | –0.276 | 2.964 | 0.045 | 3.252 | –0.288 |
| $HzPipX_2$ | 0.052 | 3.248 | 0.037 | 3.307 | -0.059 | 3.142 | 0.040 | 3.427 | -0.343 | 2.664 | 0.039 | 2.782 | –0.118 | 3.060 | 0.062 | 3.258 | –0.198 |
| B1N2 (DABNA-1) | 0.150 | 3.448 | 0.334 | 3.110 | 0.338 | 3.294 | 0.308 | 3.129 | 0.165 | 2.753 | 0.264 | 2.556 | 0.197 | 3.245 | 0.376 | 3.023 | 0.222 |
| mDBCz | 0.040 | | | | n/a | 2.792 | 0.742 | 2.753 | 0.039 | 2.050 | 0.582 | 2.021 | 0.029 | 2.636 | 0.802 | 2.754 | –0.118 |
| ν-DABNA | 0.017 | | | | n/a | 3.095 | 0.701 | 3.076 | 0.019 | 2.482 | 0.657 | 2.425 | 0.057 | 3.046 | 0.778 | 3.018 | 0.028 |

a) With the cc-pVDZ basis set. b) Vertical excitation energy at $S_0 \rightarrow S_1$ and $S_0 \rightarrow T_1$. c) Oscillator strength associated with the $S_0 \rightarrow S_1$ transition.

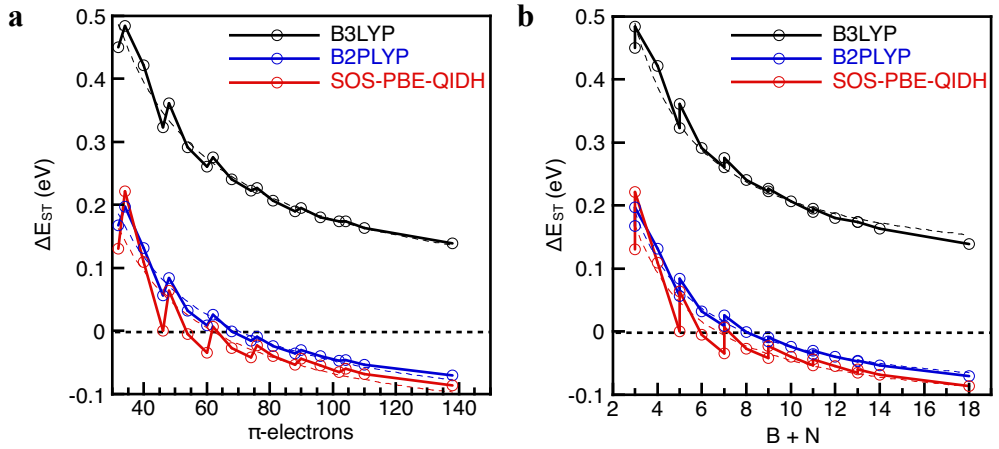


**Figure S2**. $\Delta E_{ST}$ plotted vs a) the number of π-electrons, and b) the number of B and N. The dotted lines are a curve fitting line.

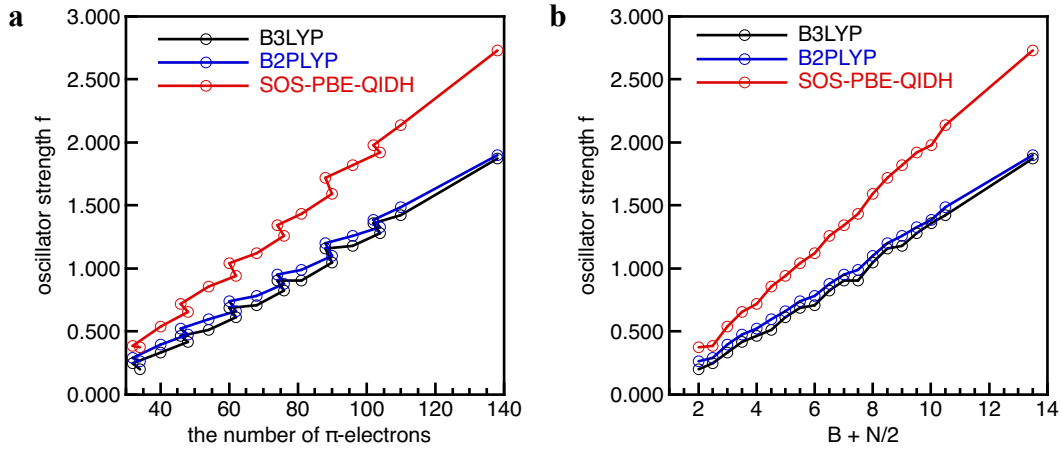


**Figure S3**. Oscillatior strength vs a) the number of π-electrons and b) sum of the number of B and half of N.

## References


1. S. Grimme, *J. Chem. Phys.*, 2006, **124**, 34108.
2. S. Grimme and F. Neese, *J. Chem. Phys.*, 2007, **127**, 154116.
3. M. Casanova-Paez and L. Goerigk, *J. Chem. Theory Comput.*, 2021, **17**, 5165.
4. M. Kondo, *Chem. Phys. Lett.*, 2022, **804**, 139895.
5. E. Bremond, J. C. Sancho-Garcia, A. J. Perez-Jimenez and C. Adamo, *J. Chem. Phys.*, 2014, **141**, 31101.
6. E. Epifanovsky, A. T. B. Gilbert, X. T. Feng, J. Lee, Y. Z. Mao, N. Mardirossian, P. Pokhilko, A. F. White, M. P. Coons, A. L. Dempwolff, Z. T. Gan, D. Hait, P. R. Horn, L. D. Jacobson, I. Kaliman, J. Kussmann, A. W. Lange, K. U. Lao, D. S. Levine, J. Liu, S. C. McKenzie, A. F. Morrison, K. D. Nanda, F. Plasser, D. R. Rehn, M. L. Vidal, Z. Q. You, Y. Zhu, B. Alam, B. J. Albrecht, A. Aldossary, E. Alguire, J. H. Andersen, V. Athavale, D. Barton, K. Begam, A. Behn, N. Bellonzi, Y. A. Bernard, E. J. Berquist, H. G. A. Burton, A. Carreras, K. Carter-Fenk,

R. Chakraborty, A. D. Chien, K. D. Closser, V. Cofer-Shabica, S. Dasgupta, M. de Wergifosse, J. Deng, M. Diedenhofen, H. Do, S. Ehlert, P. T. Fang, S. Fatehi, Q. G. Feng, T. Friedhoff, J. Gayvert, Q. H. Ge, G. Gidofalvi, M. Goldey, J. Gomes, C. E. Gonzalez-Espinoza, S. Gulania, A. O. Gunina, M. W. D. Hanson-Heine, P. H. P. Harbach, A. Hauser, M. F. Herbst, M. H. Vera, M. Hodecker, Z. C. Holden, S. Houck, X. K. Huang, K. Hui, B. C. Huynh, M. Ivanov, A. Jasz, H. Ji, H. J. Jiang, B. Kaduk, S. Kahler, K. Khistyaev, J. Kim, G. Kis, P. Klunzinger, Z. Koczor-Benda, J. H. Koh, D. Kosenkov, L. Koulias, T. Kowalczyk, C. M. Krauter, K. Kue, A. Kunitsa, T. Kus, I. Ladjanszki, A. Landau, K. V. Lawler, D. Lefrancois, S. Lehtola, R. R. Li, Y. P. Li, J. S. Liang, M. Liebenthal, H. H. Lin, Y. S. Lin, F. L. Liu, K. Y. Liu, M. Loipersberger, A. Luenser, A. Manjanath, P. Manohar, E. Mansoor, S. F. Manzer, S. P. Mao, A. V. Marenich, T. Markovich, S. Mason, S. A. Maurer, P. F. McLaughlin, M. F. S. J. Menger, J. M. Mewes, S. A. Mewes, P. Morgante, J. W. Mullinax, K. J. Oosterbaan, G. Paran, A. C. Paul, S. K. Paul, F. Pavosevic, Z. Pei, S. Prager, E. I. Proynov, A. Rak, E. Ramos-Cordoba, B. Rana, A. E. Rask, A. Rettig, R. M. Richard, F. Rob, E. Rossomme, T. Scheele, M. Scheurer, M. Schneider, N. Sergueev, S. M. Sharada, W. Skomorowski, D. W. Small, C. J. Stein, Y. C. Su, E. J. Sundstrom, Z. Tao, J. Thirman, G. J. Tornai, T. Tsuchimochi, N. M. Tubman, S. P. Veccham, O. Vydrov, J. Wenzel, J. Witte, A. Yamada, K. Yao, S. Yeganeh, S. R. Yost, A. Zech, I. Y. Zhang, X. Zhang, Y. Zhang, D. Zuev, A. Aspuru-Guzik, A. T. Bell, N. A. Besley, K. B. Bravaya, B. R. Brooks, D. Casanova, J. D. Chai, S. Coriani, C. J. Cramer, G. Cserey, A. E. DePrince, R. A. DiStasio, A. Dreuw, B. D. Dunietz, T. R. Furlani, W. A. Goddard, S. Hammes-Schiffer, T. Head-Gordon, W. J. Hehre, C. P. Hsu, T. C. Jagau, Y. S. Jung, A. Klamt, J. Kong, D. S. Lambrecht, W. Z. Liang, N. J. Mayhall, C. W. McCurdy, J. B. Neaton, C. Ochsenfeld, J. A. Parkhill, R. Peverati, V. A. Rassolov, Y. H. Shao, L. V. Slipchenko, T. Stauch, R. P. Steele, J. E. Subotnik, A. J. W. Thom, A. Tkatchenko, D. G. Truhlar, T. Van Voorhis, T. A. Wesolowski, K. B. Whaley, H. L. Woodcock, P. M. Zimmerman, S. Faraji, P. M. W. Gill, M. Head-Gordon, J. M. Herbert and A. I. Krylov, *J. Chem. Phys.*, 2021, **155**.

7. F. Furche, R. Ahlrichs, C. Hattig, W. Klopper, M. Sierka and F. Weigend, *Wiley Interdiscip. Rev. Comput. Mol. Sci.*, 2014, **4**, 91.
8. F. Neese, *Wiley Interdiscip. Rev. Comput. Mol. Sci.*, 2012, **2**, 73.
9. T. H. Dunning, *J. Chem. Phys.*, 1989, **90**, 1007.